p-ISSN 2089 – 0133 e-ISSN 2477-6416
URL: https://jurnal.uns.ac.id/ijap/article/view/106579
Indonesian Journal of Applied Physics (IJAP) Vol. 15 No.2 page 400
DOI: https://doi.org/10.13057/ijap.v15i2.106579

PERFORMANCE ANALYSIS OF EPC MATERIAL AS A KIDNEY ORGAN PHANTOM WITH EXPOSURE VOLTAGE VARIATIONS AND PA-GF-BASED KIDNEY STONE SIZE

Cari Cari, Mohtar Yunianto*, Fuad Anwar, Hardo Ardiansyah Gilang Permadi
Physics Department,Universitas Sebelas Maret, Indonesia
*mohtaryunianto@staff.uns.ac.id

Received 2025-07-21, Revised 2025-10-02, Accepted 2025-10-20,
Available Online 2025-10-20, Published Regularly October 2025

ABSTRACT

Research in the field of radiodiagnostics has been extensively developed, creating the need for substitute objects to represent human organs—namely, radiological phantoms. A phantom is a simulated model of an organ fabricated using 3D printing technology. This study aims to evaluate the suitability of Expanded Polyamide – Glass Fiber (EPA-GF) as a kidney stone phantom material embedded within a kidney phantom, based on parameters such as material density, CT number, electron density, and radiation dose across various CT scan exposure voltages. The phantom samples were printed using a dual-extruder 3D printer, with Expanded Polycarbonate (EPC) used as the kidney phantom material. CT scan exposure voltages were set to 80 kV, 100 kV, and 120 kV. Kidney stone sizes used in this study ranged from 1 mm to 8 mm (1 mm, 2 mm, 3 mm, 4 mm, 5 mm, 6 mm, 7 mm, and 8 mm). The measured density of EPA-GF was 1.51 ± 0.06 g/cm³. The CT numbers obtained at each voltage were 373.30 HU, 329.05 HU, and 299.46 HU, respectively. The corresponding electron density values were 1.231, 1.210, and 1.196, respectively. The effective doses measured at each voltage were 0.0240 mSv, 0.0448 mSv, and 0.0798 mSv. All parameter values were found to be closely aligned with literature references. The smallest visible kidney stone size detected was 2 mm.

Keywords: phantom; 3D printing; EPA-GF; kidney stone; CT number

INTRODUCTION

Kidney stone disease, or nephrolithiasis, is a condition caused by the accumulation of substances in the kidney's excretory system [1]. Kidney stones form due to a high concentration of acidic salts combined with minerals during the urine filtration process in the kidneys. The prevalence of this disease has significantly increased over the past few decades. The primary factor contributing to this rise is suspected to be the decline in individual quality of life [2].

To date, there are no definitive indicators for kidney stone disease. However, common symptoms include fatigue and frequent anxiety. According to Wang et al. (2024), significant differences are found in factors such as age, gender, race, physical condition, blood pressure, smoking status, alcohol consumption, and others [2]. One of the most commonly used diagnostic methods for kidney stones today is radiodiagnostic imaging, such as CT scans and MRI. Radiodiagnostics is a branch of radiology that uses medical imaging to diagnose diseases. This method utilizes ionizing radiation, electromagnetic waves, and charged particles to ionize the media they pass through [3]. Computed Tomography (CT) scans and Magnetic Resonance Imaging (MRI) are prominent examples of radiodiagnostic tools.

The use of phantoms in medical science is one alternative that allows for diagnostic procedures without causing harm to patients [4]. Phantoms facilitate examination by simulating human tissue, enabling accurate dose measurements while adhering to the As Low As Reasonably Achievable (ALARA) principle delivering the lowest possible radiation dose while maintaining acceptable image quality.

In terms of flexibility and cost, phantoms must meet the standards for both clinical and research applications. To address these limitations, 3D-printed phantoms offer a viable solution, as they are cost-effective and easy to manufacture [5]. With 3D printing technology, human organ shapes can be reproduced easily, and affordable filament materials can be used. Commonly used 3D printing filaments include PLA, ABS, HIPS, and PETG [6]. A 3D Print Dual Extruder is a type of printer that offers the advantage of printing with two different filaments simultaneously, making the process more efficient in both time and material usage.

Although many filament types are available for 3D printing, not all are suitable for use in kidney phantom fabrication. This is due to the requirement for the material to have an appropriate CT number (measured in Hounsfield Units, HU), which is specific to each human organ. For instance, air has a CT number of -1000 HU, the kidney ranges from 30–40 HU, the liver from 40–60 HU, and bone can reach up to 1000 HU [7], [8]. In 2016, Michiels et al. conducted a study on 3D printing materials used for proton therapy. One of the materials tested was Expanded Polyamide – Glass Fiber (EPA-GF), which yielded a CT number of 396 HU [9]. This value falls within the known CT number range for kidney stones, which is 112–1250 HU [10].

This study investigates the use of EPA-GF as a potential 3D printing filament for kidney stone phantom fabrication. The phantom samples will be printed along with Expanded Polycarbonate (EPC) as the kidney organ phantom material. The study includes variations in both kidney stone size and CT scan tube voltage (kVp). The samples will be analyzed through CT imaging to determine CT numbers, absorbed dose, material density, and relative electron density. The results will then be compared to reference parameters for kidney stones reported in the literature.

METHOD

Sample Fabrication

The test samples were designed using Autodesk Fusion 360 in the form of rectangular blocks, with size variations of 1 mm, 2 mm, 3 mm, 4 mm, 5 mm, 6 mm, 7 mm, and 8 mm. Printing was performed using a Flashforge 3D printer with 100% infill density. EPA-GF filament was used for the kidney stone samples, while EPC filament was used as the material for the kidney organ phantom.

Material Density Test

The material density was determined by measuring the mass and volume of each sample. The mass was obtained by weighing the sample using a digital balance, while the volume was measured based on the displacement of distilled water. This test was conducted to determine the density value, which represents the compactness of a substance and is expressed as the mass per unit volume. The density can be calculated using a graphical method, beginning with Equation 1 as the initial formula, and then rearranged into Equation 2.

$$\rho = \frac{m}{V} \quad (1)$$

$$m = \rho . V \quad (2)$$

It is stated that volume is the independent variable, mass is the dependent variable, and density is represented by the gradient (slope).

CT Scan Radiological Testing

The purpose of the CT scan radiological test is to obtain digital images of each sample. From these images, the CT number will be measured using the Region of Interest (ROI) technique, along with the calculation of electron density and radiation dose for each tested material.One of the properties of X-rays is their ability to penetrate materials and undergo attenuation as they pass through. The interaction between X-rays and a material causes a loss of X-ray intensity. This attenuation, or reduction in X-ray energy, depends on the material's atomic number, density, and thickness. As a result, the intensity of radiation after passing through a material is lower than the initial intensity.The resulting intensity value after X-rays pass through a material can be calculated using Equation 2, which reflects the grayscale level observed in the CT image [11].

$$I = I_0 \, e^{-\mu x} \quad (3)$$

Organs that have undergone CT scan imaging are then analyzed to obtain their corresponding CT numbers. According to Guswantoro et al. (2020), the relative electron density can be derived from the CT number values, as shown in Equations 4 and 5 below

$N_e = 1{,}052 + 0{,}00048 N_{CT}$, untuk nilai CT Number > 100 (4)

$N_e = 1{,}000 + 0{,}001 N_{CT}$, untuk nilai CT Number < 100 (5)

The effective dose received by the sample can be calculated using exposure factors and conversion values, including CTDI_{vol} (mGy), DLP (mGy·cm), SSDE (mGy), and effective dose (mSv).

The Dose Length Product (DLP) is calculated by multiplying the Computed Tomography Dose Index volume ($CTDI_{vol}$) by the scan length (L) [10]. The Size-Specific Dose Estimate (SSDE) can be obtained by multiplying the effective diameter (D_{eff}) by the size conversion factor (f) [12]. The effective diameter is derived from the anteroposterior (AP) and lateral (LAT) dimensions. AP (anteroposterior) refers to the distance from the front (anterior) to the back (posterior) of the patient's body as seen in the scanned image, while LAT (lateral) refers to the body width from the left to the right side as measured in the axial plane image. Finally, the effective dose is determined by multiplying the DLP by a region-specific conversion factor.

$$DLP = CTDI_{vol} \times L \quad (6)$$

$$SSDE = D_{eff} \times f \quad (7)$$

$$D_{eff} = \sqrt{AP \ x \ LAT} \quad (8)$$

$$E = (DLP) \times k \quad (9)$$

RESULT AND DISCUSSION

Density

The printed phantom samples were then subjected to material density testing. From the density test, mass and volume measurements were obtained. These measurement data were then processed using a graphical approximation method, applying Equation 2 to determine the density value of the samples on figure 1.

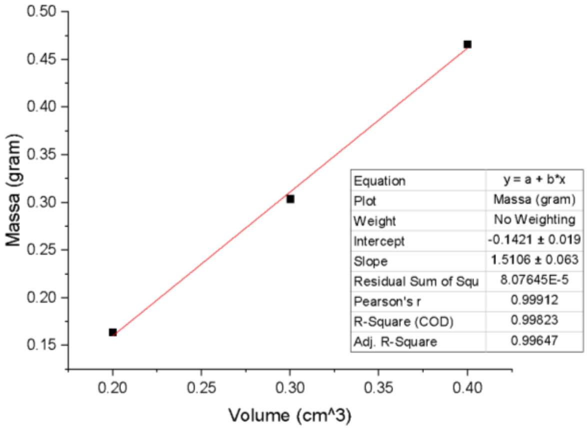

Figure 1. Graph of the Relation between Volume and Mass of EPA-GF Filament

Using the graphical method, the slope (representing the density) was obtained as 1.51 ± 0.06 g/cm³, with a coefficient of determination (R^2) of 0.99. The measured material density closely approximates the density of two types of kidney stones, with a difference of 9.9% compared to cystine stones and 11.2% compared to struvite stones [13]. When compared to data from ICRU Report 46, which lists densities of 1.660 g/cm³ for cystine stones, 1.745 g/cm³ for uric acid stones, and 2.300 g/cm³ for calcium oxalate stones, the measured density falls within a relatively close range.

CT-Number

The printed phantom samples were subsequently tested using an X-ray machine. Radiological testing was performed using X-ray exposure via a Siemens Healthineers CT Scanner, SOMATOM go.Top, serial number 120756, producing digital images in DICOM format. The CT scan images were used to determine the CT number. In this study, CT number values were obtained by defining Regions of Interest (ROI) representing grayscale intensity areas, using the RadiAnt DICOM Viewer software. The ROIs were drawn in elliptical shapes, and for each sample, nine measurement points were taken from one slice. The selected slice was the one with the clearest anatomical representation. The ROI area used for CT number determination was 0.0015 cm², corresponding to a single pixel. The ROIs created on the images displayed information such as the CT number value for the selected area. From the CT number data of each sample, a relationship can be established between the sample size variations and their respective CT number values. To understand the effect of kidney stone sample size on CT number, refer to Figure 2 below.

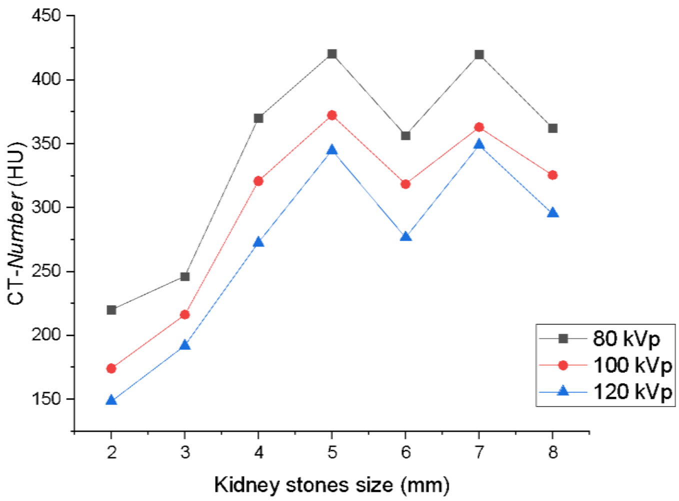

Figure 2. Graph of the Relation between Sample Size and CT-Number

An increase in tube voltage for each sample size resulted in a decrease in CT number.

This finding contrasts with the results observed in the kidney phantom, where higher tube voltages corresponded to higher CT number values. The decreasing trend of CT numbers in the kidney stone phantom as tube voltage increases is attributed to the structure of the EPA-GF material, which consists of 75% nylon and 25% glass fiber, limiting its ability to absorb radiation dose. With each increase in tube voltage, a greater amount of X-ray radiation intensity is able to penetrate the EPA-GF material, resulting in lower CT numbers. These results are consistent with findings from previous studies, where 80 kV produced a CT number of 396 HU, and 140 kV yielded 280 HU [9]. In addition to CT number values, this material behavior can also be observed through its visual appearance (visibility). By using the 3D Bone & Skin mode in RadiAnt DICOM Viewer, differences in visibility across varying tube voltages become clearly noticeable.

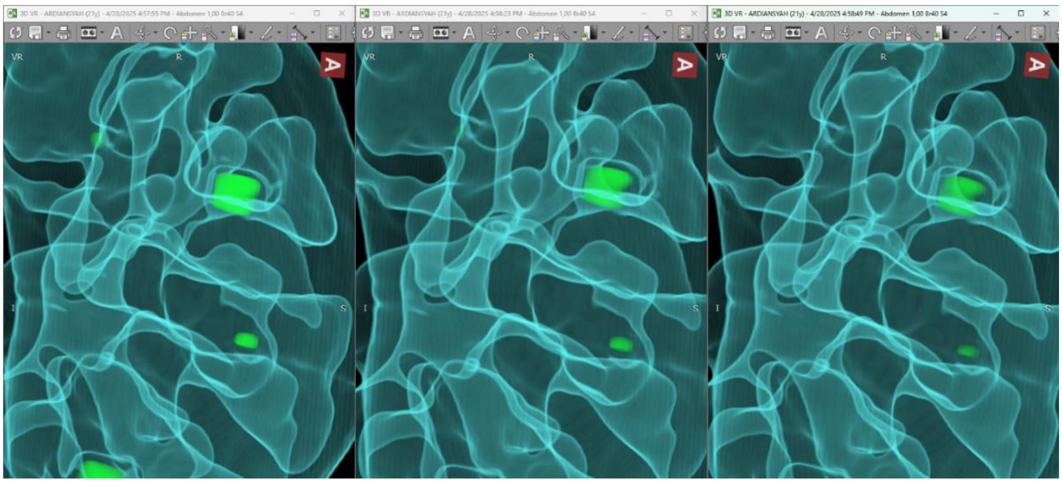

(a) (b) (c)

Figure 3. Visualization of the phantom using the 3D Bone & Skin mode in RadiAnt DICOM Viewer at varying tube voltages: (a) 80 kVp, (b) 100 kVp, and (c) 120 kVp

Figure 3 shows sample results obtained using the 3D Bone & Skin mode.This mode is a feature of RadiAnt DICOM Viewer, designed to distinguish between soft tissue and hard tissue. In the images, the green color represents hard tissue—in this case, the kidney stone phantom, while the blue color indicates soft tissue, representing the kidney phantom. As the tube voltage increases, the green color in the kidney stone phantom becomes fainter, due to the material's reduced ability to attenuate radiation at higher intensities.

The CT number reflects a material's ability to attenuate passing radiation, the thicker the material, the greater its attenuation, resulting in a higher CT number. However, in the 6 mm and 8 mm samples, a decrease in CT number compared to the 5 mm and 7 mm samples was observed. This reduction is attributed to uneven distribution of glass fiber in the filament. The 6 mm and 8 mm samples were printed earlier in the sequence, and it is likely that the filament portion used for those sizes contained less glass fiber, leading to lower attenuation capability. EPA-GF is a polyamide (PA/nylon) filament reinforced with glass fiber to improve its mechanical strength. Since glass has a higher CT number than nylon, any reduction in glass content leads to a lower overall CT number.

Overall, the CT number range for the kidney stone phantoms was 299.46 to 373.30 HU, which is considered reliable, supported by a high correlation ($R^2 = 0.987$) in the graph of tube voltage vs. CT number shown in Figure 4. When compared with reference data, EPA-GF is suitable for mimicking two types of kidney stones:

- Struvite stones, with a CT number range of 225–396 HU, and
- Calcium phosphate stones, with a range of 290–945 HU[14].

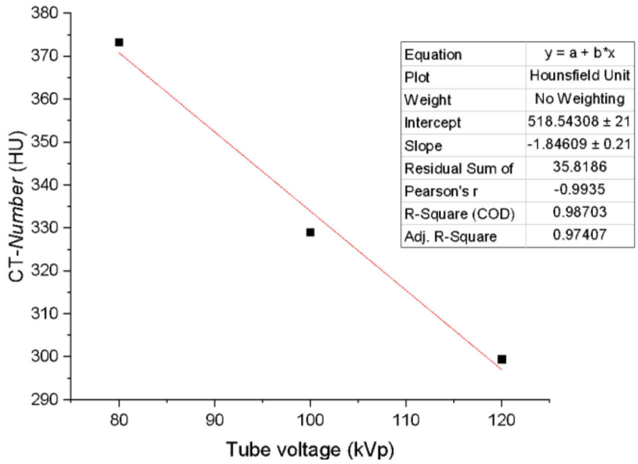

Figure 4. Plot illustrating the relation between tube voltage and CT number of the kidney stone phantom

Relative Electron Density

Relative electron density is the ratio between the electron density of a given material and that of a reference material, typically water. The relative electron density value of a sample is influenced by its corresponding CT number. By using the obtained CT number values, the relative electron density can be calculated using Equations 4 and 5.

Table 1. Calculated Electron Density Values of Phantom Samples Made from EPA-GF Material

Voltage (kVp)	Electron Denstity	Error
80	1,231	0,002
100	1,210	0,002
120	1,196	0,002

The results presented in Table 1 were compared with data from ICRU (1992), which reports relative electron densities (N_e) in the range of 1.5 to 3.0. The difference between these values and the current results is quite significant, as the ICRU data primarily represent common kidney stone types, particularly calcium oxalate, which has a CT number exceeding 1000 HU. However, when compared to references that only provide CT number values where relative electron density is calculated manually, the obtained results fall within the expected range. For example, struvite kidney stones have an electron density range of 1.160–1.242, and calcium phosphate stones range from 1.191–1.507 [14]. Thus, it can be concluded that, in terms of electron density, EPA-GF is a suitable material for use as a phantom for struvite and calcium phosphate kidney stones.

The exposure voltage (kVp) in CT scanning is closely related to electron density, since the electron density values obtained from CT scans are influenced by exposure parameters such as tube voltage (kV) and tube current (mA).The X-ray tube voltage affects both the radiation intensity and the image quality in CT scanning. The CT number represents the average X-ray attenuation in each pixel of an image, where the attenuation coefficient depends on the composition and density of the tissue. The higher the electron density in a tissue or organ, the greater the likelihood of X-ray interaction. Therefore, relative electron density plays a critical role in determining the radiation dose received by patients.

Effective Dose

In this study, the effective dose was calculated using Indose CT software by inputting the digital image data. The CT scan exposure parameters were used to determine the output dose values, namely $CTDI_{vol}$ and DLP. The Computed Tomography Dose Index Volume ($CTDI_{vol}$) represents the scanner output dose and is influenced by exposure factors. For the Wood and ASA filament samples, the $CTDI_{vol}$ was 0.44 mGy, as both were scanned using the same exposure parameters. The Dose Length Product (DLP) represents the total dose output over the scanned length and is also affected by exposure parameters.

The values of $CTDI_{vol}$, anteroposterior (AP), and lateral (LAT) dimensions were used to calculate the Size-Specific Dose Estimate (SSDE), which represents the absorbed dose by the patient or scanned object. The AP and LAT values were obtained by measuring the height (front to back) and width (left to right) of the phantom, respectively. The LAT dimension refers to the horizontal line from the left to the right boundary of the sample under measurement. As shown in Table 2, the SSDE values at 80 kV, 100 kV, and 120 kV were 0.612 mGy, 1.140 mGy, and 2.029 mGy, respectively.The size correction factor (f) for an effective diameter of 7.14 cm was determined by polynomial extrapolation based on data from AAPM Report No. 204.

Table 2. Effective Dose Values for EPA-GF Phantom Samples at Various Tube Voltages

Voltage (kVp)	LAT (cm)	AP (cm)	L (cm)	CTDIvol (mGy)	DLP (mGy·cm)	Deff	f	SSDE (mGy)	E (mSv)
80	10.44	4.88	6.09	0.22	1.340	7.14	2.78	0.612	0.0240
100	10.44	4.88	6.09	0.41	2.497	7.14	2.78	1.140	0.0448
120	10.44	4.88	6.09	0.73	4.446	7.14	2.78	2.029	0.0798

The effective dose is obtained by multiplying the measured dose with the conversion coefficient k (mSv/mGy·cm). The value of k varies depending on the body region and the patient's age. For the adult abdomen–pelvis region, the k factor is 0.01794 [15]. The effective dose values calculated at 80 kV, 100 kV, and 120 kV were 0.0240 mSv, 0.0448 mSv, and 0.0798 mSv, respectively.

The increase in dose is directly proportional to the increase in tube voltage, as higher voltages produce more electrons during the thermionic emission process. Consequently, a higher number of X-ray photons pass through the material, resulting in a greater absorbed radiation dose [16]. According to AAPM Report No. 096 (2008)[14], the typical effective dose for an abdominal CT scan is between 5 and 7 mSv. The EPC and EPA-GF materials irradiated in this study produced effective doses that are well below the standard abdominal CT dose range.

CONCLUSION

The EPA-GF-based kidney stone phantom, with a measured density of 1.51 ± 0.06 g/cm³ and CT numbers within the reference range for struvite and calcium phosphate stones, serves as an effective simulation tool for kidney stone imaging and pre-scanning procedures. The smallest visible stone size was 2 mm, as the 1 mm sample failed to provide sufficient X-ray attenuation for contrast formation. Moreover, variations in tube voltage significantly influenced CT numbers—higher voltages caused lower CT numbers and reduced image clarity. This behavior is attributed to the EPA-GF composition, containing 75% nylon and 25% glass fiber, which limits radiation absorption.

ACKNOWLEDGMENT

The author would like to thank LPPM UNS for providing funding through the 2025 Research Group Grant with contract number 371/UN27.22/PT.01.03/2025.

REFERENCES

[1] X. Zheng, Y. Wu, L. Huang, and J. Xiong, “Trajectories of body mass index and incident kidney stone disease: a prospective cohort study in Chinese young adults,” *Urolithiasis*, vol. 52, no. 1, p. 118, Aug. 2024, doi: 10.1007/s00240-024-01617-9.

[2] M. Wang *et al.*, “Association of health-related quality of life with urinary tract infection among kidney stone formers,” *Urolithiasis*, vol. 52, no. 1, p. 103, July 2024, doi: 10.1007/s00240-024-01601-3.

[3] H. Nurvan et. ,. al., “Radiology as a support for examination and treatment in the medical world and its effects: literature review,” *Sci. Midwifery*, vol. 11, no. 3, 2023.

[4] C. Stengl *et al.*, “A phantom to simulate organ motion and its effect on dose distribution in carbon ion therapy for pancreatic cancer,” *Phys. Med. Biol.*, vol. 68, no. 24, p. 245013, Dec. 2023, doi: 10.1088/1361-6560/ad0902.

[5] L. Jessen, J. Gustafsson, M. Ljungberg, S. Curkic-Kapidzic, M. Imsirovic, and K. Sjögreen-Gleisner, “3D printed non-uniform anthropomorphic phantoms for quantitative SPECT,” *EJNMMI Phys.*, vol. 11, no. 1, p. 8, Jan. 2024, doi: 10.1186/s40658-024-00613-7.

[6] A. Al Rashid, S. A. Khan, S. G. Al-Ghamdi, and M. Koç, “Additive manufacturing of polymer nanocomposites: Needs and challenges in materials, processes, and applications,” *J. Mater. Res. Technol.*, vol. 14, pp. 910–941, Sept. 2021, doi: 10.1016/j.jmrt.2021.07.016.

[7] N. L. Q. Cuong, N. H. Minh, H. M. Cuong, P. N. Quoc, N. H. V. Anh, and N. V. Hieu, "Porosity Estimation from High Resolution CT SCAN Images of Rock Samples by Using Housfield Unit," *Open J. Geol.*, vol. 08, no. 10, pp. 1019–1026, 2018, doi: 10.4236/ojg.2018.810061.
[8] Z. Xiao, B. Liu, L. Geng, F. Zhang, and Y. Liu, "Segmentation of Lung Nodules Using Improved 3D-UNet Neural Network," *Symmetry*, vol. 12, no. 11, p. 1787, Oct. 2020, doi: 10.3390/sym12111787.
[9] S. Michiels *et al.*, "Towards 3D printed multifunctional immobilization for proton therapy: Initial materials characterization," *Med. Phys.*, vol. 43, no. 10, pp. 5392–5402, Oct. 2016, doi: 10.1118/1.4962033.
[10] P. Dio, C. Anam, and E. Hidayanto, "Comparison of Central, Peripheral and Weighted Size Specific Dose in CT to Dose Results from IndoseCT Software," *Int. J. Res. Rev.*, vol. 9, no. 7, pp. 249–253, July 2022, doi: 10.52403/ijrr.20220729.
[11] T. Meilinda et. ,. al., "Pengaruh perubahan faktor eksposi terhadap nilai CT number," *Youngster Phys. J.*, vol. 3, no. 3, 2014.
[12] C. et. al. Anam, "IndoseCT Software for Calculating and Managing Radiation Dose of Computed Tomography for an Individual Patient. Indonesia," *Diponegoro Univ.*.
[13] B. Yang, A. Ray, J. Zhang, and B. Turney, "Quartz sand as a phantom for urinary stone dust," *BJU Int.*, vol. 136, no. 3, pp. 417–419, Sept. 2025, doi: 10.1111/bju.16810.
[14] P. S. et. al. Shahnani, "The comparative survey of Hounsfield units of stone composition in urolithiasis patients," *J. Res. Med. Sci. Off. J. Isfahan Univ. Med. Sci.*, vol. 19, no. 7, 2014.
[15] C. De Mattia *et al.*, "Patient organ and effective dose estimation in CT: comparison of four software applications," *Eur. Radiol. Exp.*, vol. 4, no. 1, p. 14, Dec. 2020, doi: 10.1186/s41747-019-0130-5.
[16] F. Fiarka, S. Oktamuliani, and N. Nuraeni, "Pengaruh Tegangan terhadap Nilai CTDIvol, Dose Length Product dan Dosis Efektif pada Pemeriksaan Computed Tomography (CT) Abdomen: Studi di Rumah Sakit Umum Pusat Dr. M. Djamil," *J. Fis. Unand*, vol. 12, no. 4, pp. 591–597, Oct. 2023, doi: 10.25077/jfu.12.4.591-597.2023.